Applied Mathematical Modelling 37 (2013) 137–154

Contents lists available at SciVerse ScienceDirect

Applied Mathematical Modelling

journal homepage: www.elsevier.com/locate/apm

Aircraft proximity termination conditions in the planar turn centric modes

Union H.-N. Huynh, Neale L. Fulton *

Division of Mathematics, Informatics and Statistics, Commonwealth Scientific and Industrial Research Organisation, G.P.O. Box 664, Canberra, ACT 2601, Australia

ARTICLE INFO

Article history:
Received 4 December 2009
Received in revised form 5 December 2011
Accepted 12 December 2011
Available online 15 February 2012

Keywords:
Collision avoidance
Cooperative manoeuvres
Fixed reference point
Optimisation
Turn rates
Proximate

ABSTRACT

Closed-form analytic solutions for proximity management strategies are of great importance as a design benchmark when validating both automated systems and procedures associated with the design of air traffic rules. Merz (1973) first presented a solution for a set of optimal strategies for resolving co-planar co-operative encounters between two aircraft (or ships) with identical linear and rotational speeds. This paper extends the solution domain for turning aircraft beyond that of identical aircraft by presenting a rigorous analysis of the problem through a generalised optimisation approach. This analysis provides a dependable method for determining the location of the point of closest approach. This is achieved by using a vector form of Fermat's equation for stationary points. A characteristic of this solution is the identification of a fixed reference point lying on the vector between the aircraft turn centres or on one of its extensions. This point is then used to determine where the location of the minima in the relative range between the aircraft will occur. Bounds for the domain of the solution are constructed in terms of the rotational angles of the aircraft on their turn circles. Four distinct topologies are required to characterise the types of minima that can occur. The methodology has applications in an operational context permitting a more detailed and precise specification of proximity management functions when developing algorithms for aircraft avionics and air traffic management systems.

1. Introduction

Systems that provide aircraft proximity management functions are currently under intensive review. This is due to the expected increase in traffic flow rates from three major areas: public demand for air travel, the introduction of uninhabited aerial vehicle operations (without a human pilot) and from the introduction of personalised jets. Concomitant with these increases is an expected increase in the frequency of aircraft proximity incidents. Close proximity situations can occur, for example, in the missed approach, in the circuit area, and for operations in uncontrolled airspace where aircraft routinely fly in close proximity and where air traffic management (ATM) services may be unavailable. These situations require dependable proximity management at physical limits well below the more commonly understood ATM separation standards used in the present controlled airspace and well below those presently proposed for situations such as Free Flight airspace. The assurances that minimum miss-distances as well as available response times will be preserved during close proximity situations are important objectives for engineering design (Refs. [1,2]) and for the conduct of flight operations (Refs. [3,4]).

The need for this research also arises within the airspace planning groups. Programmes such as NextGen in the USA and SESAR in Europe will require at least some re-design and validation of both conflict resolution and proximity management functions. Further, aircraft guidance that enhances the tracking and the prediction of flight paths is being investigated under new avionics architectures such as: "Pathway-in-the-Sky", "Tunnel-in-the-Sky", "Highway-in-the-Sky" (Refs. [5–15]) and "Cockpit Display for Traffic Information (CDTI)" initiatives (Refs. [16–20]).

* Corresponding author.
E-mail address: neale.fulton@csiro.au (N.L. Fulton).

0307-904X/$ - see front matter © 2012 Elsevier Inc. All rights reserved.
doi:10.1016/j.apm.2011.12.045

Nomenclature

a	turn radius of aircraft-*A*
b	turn radius of aircraft-*B*
$r = \frac{a}{b}$	ratio of turn radii (a non-dimensional quantity)
R	relative range from aircraft-*A* to aircraft-*B*
t	time variable
ζ	rotational angle of aircraft-*A*
γ	rotational angle of aircraft-*B*
ζ_0	initial angle of aircraft-*A*
γ_0	initial angle of aircraft-*B*
ζ^*	optimal rotational angle of aircraft-*A*
γ^*	optimal rotational angle of aircraft-*B*
$\omega_A, \underline{\omega}_A$	rotational speed (velocity) of aircraft-*A*
$\omega_B, \underline{\omega}_B$	rotational speed (velocity) of aircraft-*B*
$\omega = \frac{\omega_A}{\omega_B}$	ratio of rotational speeds (a non-dimensional quantity)
*Arc*sin (•)	principal value of the inverse sine
*Arc*tan (•)	principal value of the inverse tangent
$\boldsymbol{C}_A$	turning circle of aircraft-*A*
$\boldsymbol{C}_B$	turning circle of aircraft-*B*
$\underline{C}$	turn centre vector of turn circles from aircraft-*A* to aircraft-*B*
$C = \|\underline{C}\|$	turn centre distance
$\|\bullet\|$	the L_2 or Euclidean Norm of a vector
$m \ll n$	the magnitude of m is much, much less than the magnitude of n

All of these initiatives will require a refinement of the *Rules of the Air* by which aircraft manage proximity and by which collision risk is minimised. Such refinement needs to be based on a much improved understanding of the required optimal behaviour when aircraft are manoeuvring in close proximity. Rigorous models are therefore required to consolidate and extend the physical and mathematical foundation on which the present *Rules of the Air* are based and on which new rules may be constructed. Further background is provided in Ref. [21] as to the international development in ATM systems, and as to the engineering processes required based on both rigorous mathematics and formal methods. The most significant observation is that in the design of real, complex engineering systems it is not always possible to achieve the goal of finding closed-form solutions to a problem but the engineering imperative is always to seek to do so. We pursue this imperative in this paper.

A more precise specification of the location of the point of closest approach (PCA) between the trajectories of two vehicles, together with its associated evaluation of a miss distance, *D*, are important and necessary requirements for managing close proximity and for resolving conflict situations for both aircraft and ships (Refs. [22–32]). A common implementation has been to use D_{SS} the estimated minimum 3D miss-distance between the linear extrapolations of the instantaneous velocity vectors of two vehicles. This specific measure has had long standing within the aerospace industry (Refs. [3,4,23,27,33–37]). It is also identified within the international literature as the basis of various guidance laws (Refs. [23,27,34,35]).

However, in some situations D_{SS} may not be the appropriate measure to use. Such a case is during the simultaneous arrival of two aircraft to parallel runways. One aircraft can be on a left base for the left runway, the other on a right base for the right runway each flying a mirror-symmetric flight-path to the other. In this situation D_{SS} is zero for some duration in the turns yet operations are normal. Similar situations arise within the circuit area where aircraft turn circles are established in close proximity by well defined and prescribed spatial procedures. In these circumstances pilots need to be able to dynamically predict the miss distance, D_{TT}, between both aircraft while turning, and where this will occur in the turn, PCA_{TT} (not PCA_{SS}). This measure has been the subject of studies on the optimal resolution of both ship and of aircraft conflicts (Refs. [22–32]). While considerable advances based on numerical optimization techniques have been made making it possible to study complex scenarios involving many participants, the fact remains that the underlying mathematical essence has not be fully recovered. It is therefore important that such results be validated against analytic or semi-analytic syntheses of optimal solutions for realistic scenarios. To this end the research of this paper refines and elaborates the specification of the termination conditions found in Refs. [3,4,36], by removing the constraints of both a unity speed ratio and a unity turn-rate ratio thus augmenting the rigorous specification of termination conditions as found in Ref. [21]. Four fundamental cases for the termination criteria are identified and then examined with the intent of contributing to a suite of mathematical models that will more adequately support the assessment of performance and the validation of both the present *Rules of the Air* and of future proximity management procedures and systems.

1.1. Domain of the problem

The situation where two aircraft are both turning in close proximity is considered. The specific problem is to specify the nature of the spatial termination criteria under which PCA_{TT} occurs for the planar, non-intersecting turn-centric mode.

A state-vector $\rho = (R, \phi, \theta)$ specifies the instantaneous relative position in polar coordinates (R, ϕ) and the relative heading, θ, the instantaneous relative direction of motion being the difference between the two aircraft headings. The relative range between aircraft is $\boldsymbol{R}$ expressed as a function of five independent variables:

1. $\boldsymbol{C}$ – the distance between the turn centres of the aircraft,
2. a and b – the individual turn radii, and
3. υ and ω – the two parameters of the problem, that represent the ratio of the linear speeds and the ratio of the maximum turn rates, respectively. Note that in this formulation of the problem ω can be a signed quantity and that υ can be non-unity.

The domain of υ and ω can be characterized via the Cartesian product:

$$\Gamma \times \Omega = \{(\upsilon, \omega) : \upsilon \in \Gamma, \omega \in \Omega; \quad \Gamma \subset \boldsymbol{R}, \Omega \subset \boldsymbol{R}\}$$

We note that there is a choice in the selection of parameters and equally r and ω could have been chosen, which, in that case, would represent the ratios of the turn radii and of the turn rates, respectively. The domain of the parameters of the problem would then have been characterized as:

$$\mathrm{P} \times \Omega = \{(r, \omega) : r \in \mathrm{P}, \omega \in \Omega; \quad \mathrm{P} \subset \boldsymbol{R}, \Omega \subset \boldsymbol{R}\}$$

An important example of the problem of this paper was first studied by Merz (Refs. [3,4]) for $\upsilon = 1$, $\omega = 1$ (aircraft or ships of identical speed and turn capabilities). A more rigorous analysis is presented in Ref. [36] while Ref. [37] extends the Merz case to the situation in which the aircraft have different turn capabilities (i.e., $\upsilon = 1$, $\omega > 0$). In Refs. [36,37] $\upsilon = 1$ and therefore $\frac{1}{r} \leqslant \omega \leqslant r$ where r is the ratio of the turn radii. The serious limitation of "identical aircraft" in which the respective turn radii and turn speeds are identical are removed in the present paper. In an operational context typical bounds and constraints can be placed on the parameters as follows.

The turn rates for individual aircraft can vary significantly from zero (in straight flight) to over 90 degrees/s in a tight turn. Thus, in general the turn rate ratio, ω, is such that $0 \leqslant |\omega| < \infty$.

The turn radii are positive and finite, specified as $0 < a, b < \infty$. There is a minimum feasible turn radius for a given aircraft, but the actual radii achieved are dependent on the aircraft configuration (position of the flaps and the landing gear); design limitations imposed on the angle of bank (e.g., 60 degrees is common); and on the true airspeed at the time of banking. Broad consideration of these factors would suggest that the turn radii will typically fall in the range of a few metres to 30 km. The case of an infinite turn radius (with ownaircraft travelling in a straight line, the intruder circling) is addressed in Ref. [38].

To conclude this section we draw upon the research of Park, Deyst and How (Ref. [39]) who demonstrated guidance logic to control unmanned aerial vehicles when flying in a circle. In this trial the radius was ca. 250 m, with an aircraft controlled to within 1.6 m RMS while flying the circular path. The same logic was used for air rendezvous bringing the aircraft to within 12 m separation with 1.4 m RMS relative position error. The precision of navigation achieved in this experiment provides a pragmatic context for the research of this paper. The most general situation between two aircraft both turning in a plane in close proximity ($0 \leqslant \upsilon < \infty$ and $0 \leqslant |\omega| < \infty$) is now considered.

1.2. The mathematical approach

The strategy of solution presented in the paper is based on three stages, the first two of which are straightforward.

Stage 1: The problem is first cast in terms of the square of the relative range, R, (the distance along the line of sight between the aircraft).

Stage 2: Fermat's method for Stationary Points (Refs. [40–43]) is applied. This leads to complex transcendental equations but since the starting point is the square of R one might expect a linear relationship to be embedded in the solution. The identification and specific characterisation of this relationship is a novel aspect of this research (as reported in Ref. [21]). It is important because its discovery permits a direct link to be made between the geometrical (operational) situation and the vector formulation. It permits a more intuitive and direct identification of four special categories of minima that can arise in real operations. These categories subsequently require careful attention in the development of both the rigorous and formal proofs that underpin the design of proximity management systems. This level of attention to detail is required so that these systems will continue to function correctly in all operational situations that might be encountered.

Stage 3: The linear relationship can be made explicit by casting the transcendental equation for R^2 in the form of a vector equation. A novel feature in the construction is that ***a fixed reference point*** for stationary states, F, is identified that lies on the vector between the aircraft turn centres or on one of its extensions. This brings new insight as to an invariant geometrical condition under which a minimum in relative range will occur and thus brings further utility as to how to best test such systems from a safety critical systems perspective.

The point, F, is used to determine the location of the minima in relative range, $\mathrm{PCA}_{\mathrm{TT}}$, between the aircraft. Bounds in terms of the rotational angles of the aircraft on their turn circles are constructed for the domain of the solution for $\mathrm{PCA}_{\mathrm{TT}}$.

The minima are characterized by four distinct topologies: a global minimum (M_0); a parallel minimum (M_1); a radial minimum (M_2); and a transverse minimum (M_3). Straightforward procedures for calculating the closed form solutions are presented.

The remainder of this paper is organized as follows:

Section 2: Formulation of the optimisation problem.
Section 3: Geometrical relations associated with stationary points.
Section 4: Categorisation of the minima.
Section 5: Sufficient condition for determination of aircraft miss-distances.

2. Formulation of the optimisation problem

2.1. Conventions and their application

One of the most common earth reference coordinate frames in aerospace design is that of the North, East, Down (NED) frame (Ref. [44]). This frame has been established to facilitate the navigation of aircraft over the earth's surface. Two of its axes are embedded in the local earth tangential plane, and the direction of the third is derived by application of vector cross product to the North and East vectors respectively. However, while this is a very common co-ordinate system it may not be the best system in which to derive a tractable closed form solution for the candidate problem. For this reason a new co-ordinate system was defined that simplifies the problem and assures tractability. It is a routine engineering procedure to translate from one coordinate frame to another as may be required in an actual system design. We also note that the NED coordinate system embraces the convention of compass degrees, whereas our selection of coordinate system remains with the standard mathematical convention of angular measure. This choice is deliberate to ensure that mathematical conventions embodied in the specifications of the circular functions and their inverses are more easily respected throughout the derivation. Again it is a matter of simple transformation to adapt the conventions on which the solution is based to the alternative compass paradigm. Finally, in the derivations that follow, we make explicit, and distinguish, the cases such as $a < b$ and $b < a$. This is because during actual operations of a specified aircraft navigation system (ownaircraft versus an intruder) it will not be known *a priori* which particular case will be encountered. Both must be accommodated in the design as the algebraic approach and the numerical conditions required for solution may be quite different for each case and role.

2.2. The planar turn centric mode

We now pose the problem in earth coordinates as shown in Fig. 1. Two aircraft are turning uniformly in a planar turn centric mode. The coordinate system's origin is set at point O_A, the centre of aircraft-A's turning circle, $\mathbf{C}_A$. The X axis is aligned parallel to, and coincident with, the line (O_AO_B) joining the centres of each aircraft's turn circle. The Y axis is set perpendicular to the X axis at O_A. The Z axis is constructed by the Right-Hand rule to be perpendicular to the turning plane $(\overrightarrow{O_AX}, \overrightarrow{O_AY})$ at the origin O_A as shown in Fig. 1. By mathematical convention, the positive direction of increasing angles is represented by a left (anti-clockwise) turn. The angle, ζ, has its vertex at O_A, and is measured from the reference $\overrightarrow{O_AX}$. Similarly, the angle, γ, has its vertex at the centre O_B, and is measured from the reference $\overrightarrow{O_BX}$. The angular turn rates, ω_A, and, ω_B, for aircraft-A and B respectively, are independent constants. Both phase angles, ζ and γ, are linear functions of time with initial values: ζ_0 and γ_0. Thus,

$$\begin{cases} \zeta = \omega_A t + \zeta_0 \\ \gamma = \omega_B t + \gamma_0 \end{cases}$$

Let a and b be the radii of the turning circles C_A and C_B respectively.

Let

$$\underline{C} = \overrightarrow{O_AO_B} \Rightarrow \underline{C} = \|\underline{C}\|$$
$$\underline{a} = \overrightarrow{O_AP_A} \Rightarrow a = \|\underline{a}\|$$
$$\underline{b} = \overrightarrow{O_BP_B} \Rightarrow b = \|\underline{b}\|$$
$$P_A = (x_A, y_A) = (a\cos\zeta, a\sin\zeta)$$
$$P_B = (x_B, y_B) = (C + b\cos\gamma, b\sin\gamma)$$
$$\underline{R} = \overrightarrow{P_AP_B} \Rightarrow R = \|\underline{R}\| = \sqrt{(x_A - x_B)^2 + (y_A - y_B)^2}$$

Given the instantaneous turn-radius vectors $\underline{a}$ and $\underline{b}$, and the known turn-centre vector $\underline{C}$ then the relative range vector, $\underline{R}$, can be expressed as:

$$\underline{R} = \underline{C} - \underline{a} + \underline{b}$$

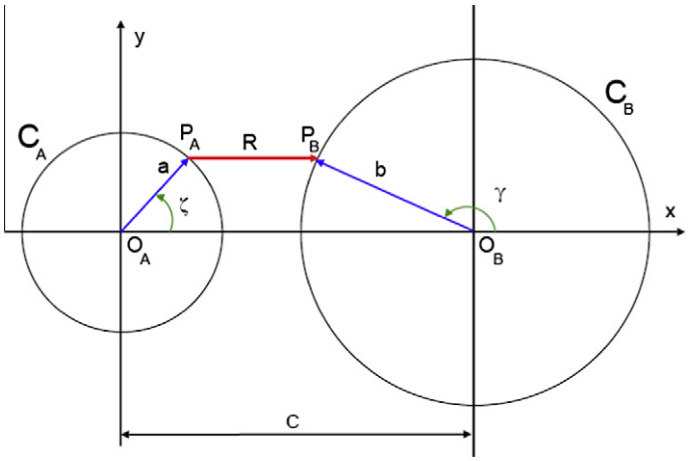

Fig. 1. Cartesian coordinate system.

$$\Rightarrow \quad R = \begin{bmatrix} R_X \\ R_Y \end{bmatrix} = \begin{bmatrix} C \\ 0 \end{bmatrix} - \begin{bmatrix} a\cos\zeta \\ a\sin\zeta \end{bmatrix} + \begin{bmatrix} b\cos\gamma \\ b\sin\gamma \end{bmatrix} = \begin{bmatrix} C - a\cos\zeta + b\cos\gamma \\ b\sin\gamma - a\sin\zeta \end{bmatrix}$$

$$\Rightarrow \quad R^2 = C^2 + a^2 + b^2 - 2Ca\cos\zeta + 2Cb\cos\gamma - 2ab\cos(\zeta - \gamma) \tag{1}$$

3. Geometrical relations associated with the stationary points

Expressions for the geometrical relations between the aircraft positions are derived in this section and a classification of the possible proximity termination conditions presented.

It is of interest to find the pair of phase angles (ζ^*, γ^*) so as to minimise R^2. This is a nonlinear and unconstrained optimisation problem in the two time dependent variables ζ and γ. The problem can be solved by a formulation of Fermat's method for stationary points (Refs. [40–43]). The method generally depends in its expression on the total differential (Refs. [45,46]), as cast, in this case, with respect to the phase angles. However, due to the temporal dependency of each phase angle the total derivative (Ref. [47]) of the function R^2 is required to determine the stationary points and to extract the nature of the solution.

3.1. Fermat's vector equation and the fixed reference point

Assume that the two angular velocities (ω_A, ω_B) are given together with the geometry of the two turning circles. Then, the relative range vector is written as: $\underline{R} = \underline{C} + \underline{b} - \underline{a}$

$\Rightarrow \dot{\underline{R}} = \dot{\underline{b}} - \dot{\underline{a}}$ where the over-dot represents the $\frac{d(.)}{dt}$ operator and $\underline{C}$ is constant,

$$\text{with } \dot{\underline{R}} = \frac{d\underline{R}}{dt}$$

$$\dot{\underline{a}} = \frac{d\underline{a}}{dt} = (-\omega_A a\sin\zeta,\ \omega_A a\cos\zeta) \text{ by } \underline{a} = (a\cos\zeta, a\sin\zeta)$$

$$\dot{\underline{b}} = \frac{d\underline{b}}{dt} = (-\omega_B b\sin\gamma, \omega_B b\cos\gamma) \text{ by } \underline{b} = (b\cos\gamma, b\sin\gamma)$$

$\Rightarrow \frac{dR^2}{dt} = 2\dot{\underline{R}}\cdot\underline{R} = 2(\dot{\underline{b}} - \dot{\underline{a}})\cdot\underline{R}.$

Fermat's method for stationary points (Refs. [40–43]) states that the stationary points of R^2 can be found as the roots of the following equation:

$$\frac{dR^2}{dt} = 0$$

Fermat's vector equation for the stationary points now becomes:

$$(\dot{\underline{b}} - \dot{\underline{a}})\cdot\underline{R} = 0$$

Clearly, at the stationary points, the vector $(\dot{\underline{b}} - \dot{\underline{a}})$ is orthogonal to the vector $\underline{R}$. In this particular case, by inspection, vector $(\omega_B \underline{b} - \omega_A \underline{a})$ is also orthogonal to the vector $(\dot{\underline{b}} - \dot{\underline{a}})$. Thus, in the planar case, $(\omega_B \underline{b} - \omega_A \underline{a})$ is parallel to $\underline{R}$. Then, Fermat's vector equation, written in a general form, is:

$$(\omega_B \underline{b} - \omega_A \underline{a}) \times \underline{R} = 0 \Rightarrow [\omega_B(\underline{R} - \underline{C} + \underline{a}) - \omega_A \underline{a}] \times \underline{R} = 0 \text{ by } \underline{b} = \underline{R} - \underline{C} + \underline{a} \tag{2}$$

Reducing Eq. (2) we obtain:

$$[\omega_B \underline{C} + (\omega_A - \omega_B)\underline{a}] \times \underline{R} = 0 \tag{3}$$

A number of special cases of Eq. (3) provide further insight as to the fundamental relationships involved.

If $\omega_B = 0$, then Eq. (3) becomes:

$$\underline{a} \times \underline{R} = 0 \text{ (provided } \omega_A \neq 0) \Rightarrow O_A,\ P_A \text{ and } P_B \text{ are collinear.}$$

If $\omega_B \neq 0$, then Eq. (3) can be represented in the form of:

$$[\underline{C} - (1 - \omega)\underline{a}] \times \underline{R} = 0 \quad \text{where } \omega = \frac{\omega_A}{\omega_B}$$

If $\omega = 1$, then Eq. (3) is reduced to:

$$\underline{C} \times \underline{R} = 0 \Rightarrow \underline{C} \text{ and } \underline{R} \text{ are parallel.}$$

Otherwise, for $\omega \neq 1$ and finite, then Eq. (3) can be written as:

$$\left[\left(\frac{1}{1-\omega}\right)\underline{C} - \underline{a}\right] \times \underline{R} = 0 \tag{4}$$

Interpretation of Eq. (4) shows that the straight lines generated by the vectors $\underline{R}$ and $\underline{C}$ are transverse and intersect at a fixed reference point, F, corresponding to a specific value of ω. Then F is given by $\left(\frac{C}{1-\omega}, 0\right)$. The importance of this result is that when the point, F is determined it can then be used to construct the aircraft positions at which the minimum of R^2 will occur. A corollary of this property is that, in general, aside from the few special cases, the points P_A, P_B and F will be collinear at the minimum relative range.

A further case of interest is when $\omega_A = -\omega_B$ then $\omega = -1$, and then F is $\left(\frac{C}{2}, 0\right)$, the midpoint of the turning centres O_A and O_B.

If $\omega_A = 0$ then the point F is located at O_B, and if $\omega_B = 0$ then F is located at O_A.

We can also prove for $\omega < 0$ that F will be an interior point of the interval joining the turning centres, $O_A O_B$. The length of the interval $O_A O_B$ is always equal to C and F will be an interior point of this interval, if and only if

$$\begin{aligned} 0 < \tfrac{C}{1-\omega} < C \quad &\Longleftrightarrow \quad 0 < \tfrac{1}{1-\omega} < 1 \text{ by } C > 0 \\ &\Longleftrightarrow \quad 1 < 1 - \omega \\ &\Longleftrightarrow \quad \omega < 0 \end{aligned}$$

Finally, and inversely, for $\omega > 0$, it is possible to verify that F will be located on the straight line generated by vector $\underline{C}$ and exterior to the interval $O_A O_B$.

Several important conclusions from this section are as follows:

1. the fixed reference point for stationary states F is a function of ω,
2. if $\omega = 0$, that is, $\omega_A = 0$, the point F will coincide with the centre O_B,
3. if $\omega = \infty$, that is, $\omega_B = 0$, the point F will coincide with the centre O_A, and
4. the sign of ω determines where the point F will be spatially located in relation to the two turning centres O_A and O_B (for ω negative, the point F will be an interior point of the interval $O_A O_B$. Otherwise, if ω positive, it will be located outside that interval).

3.2. Bounds on the solution domain for the minima

The positions of the two aircraft and the vector $\underline{R}$ are always determined by reference to the pair (ζ, γ). The solution domain expressed through this pair is bounded since our interest is only in the pairs for which a minimum occurs. This permits attention to be restricted to those regions of $\mathbf{C}_A$ and $\mathbf{C}_B$ that are delimited by the two inner and the two outer common tangents.

The process followed in this section also shows that two further points on the extension of the interval $O_A O_B$ are important in the construction of a solution. These points are, respectively, I and J being the intersection points of the two inner and the two outer common tangents to the two turning circles. By symmetry of the tangents with respect to the line joining the turning centres, all points: J, O_A, I and O_B are collinear. Their order on the X axis is established by the relative size of the radius a with respect to the radius b.

A number of special sets of (ζ,γ) can then be identified that satisfy the requirements as the domain in which the minimum of R^2 occurs. In the following, an algorithm to determine all such possible domains is discussed.

3.2.1. Case a < b

In the case of $a < b$, and by symmetry of the tangents with respect to C, all points: J, O_A, I and O_B are collinear and are established on the X axis in this order. From Fig. 2, we obtain: $I = \left(\frac{aC}{a+b}, 0\right)$ and $J = \left(\frac{aC}{a-b}, 0\right)$. Clearly, points I and J can be determined by the radii and turning centres as fixed reference points.

There are three possible cases for the location of the fixed reference point F:

(i) When F is located on the left hand side of point J, we have

$$\frac{C}{1-\omega} \leqslant \frac{aC}{a-b}$$

$$\Rightarrow \quad \frac{1}{1-\omega} \leqslant \frac{a}{a-b} \ (\text{by } C>0)$$

$$\Rightarrow \quad \frac{1}{1-\omega} \leqslant \frac{1}{1-\frac{1}{r}} \ \left(\text{where } r = \frac{a}{b} > 0\right)$$

In this case the phase angle ζ is bounded by the two tangents constructed from point $\left(\frac{C}{1-\omega}, 0\right)$ to $\boldsymbol{C}_A$. Thus, from Fig. 2, $|\zeta| \leqslant \bar{\zeta}$, where $\bar{\zeta}$ be the absolute bound of ζ. By Trigonometry, we have

$$\sin\left(\bar{\zeta} - \frac{\pi}{2}\right) = \frac{a}{\frac{C}{(1-\omega)}} = \frac{a(1-\omega)}{C} \ (\text{see Fig. 2})$$

$$\Rightarrow \quad |\zeta| \leqslant \frac{\pi}{2} + Arc\sin\left(\frac{a(1-\omega)}{C}\right)$$

(ii) When F is located between points J and I, that is: $\frac{aC}{a-b} \leqslant \frac{C}{1-\omega} \leqslant \frac{aC}{a+b}$

$$\Rightarrow \quad \frac{a}{a-b} \leqslant \frac{1}{1-\omega} \leqslant \frac{a}{a+b} \ (\text{by } C>0)$$

$$\Rightarrow \quad \frac{1}{1-\frac{1}{r}} \leqslant \frac{1}{1-\omega} \leqslant \frac{1}{1+\frac{1}{r}} \quad \left(\text{where } r = \frac{a}{b} > 0\right)$$

In this case the phase angle γ, is bounded by the two tangents, constructed from point $\left(\frac{C}{1-\omega}, 0\right)$ to $\boldsymbol{C}_B$. Similarly, Fig. 2 gives: $\frac{\pi}{2} + \bar{\gamma} \leqslant \gamma \leqslant \frac{3\pi}{2} - \bar{\gamma}$, where $\sin(\bar{\gamma}) = \frac{b}{\frac{C}{(1-\omega)}} = \frac{b(1-\omega)}{C}$

$$\Rightarrow \quad \frac{\pi}{2} + Arc\sin\left(\frac{b(\omega-1)}{\omega C}\right) \leqslant \gamma \leqslant \frac{3\pi}{2} - Arc\sin\left(\frac{b(\omega-1)}{\omega C}\right)$$

(iii) When F is located on the right hand side of point I, then: $\frac{aC}{a+b} \leqslant \frac{C}{1-\omega}$.

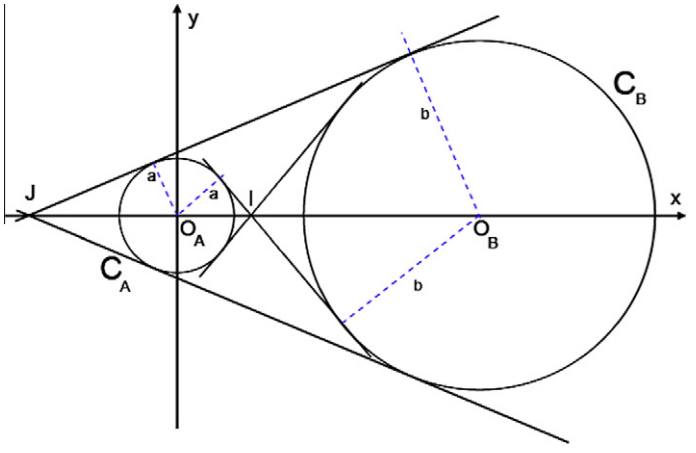

Fig. 2. Geometry for fixed reference points I and J.

$$\Rightarrow \quad \frac{a}{a+b} \leqslant \frac{1}{1-\omega} \ (\text{by } C > 0)$$

$$\Rightarrow \quad \frac{1}{1+\frac{1}{r}} \leqslant \frac{1}{1-\omega} \quad \left(\text{where } r = \frac{a}{b} > 0\right)$$

In this case the phase angle ζ is again bounded by the two tangents constructed from point $(\frac{C}{1-\omega}, 0)$ to $\boldsymbol{C}_A$. By using similar logic, as in Section 3.2.1 (i), we find that:

$$|\zeta| \leqslant \frac{\pi}{2} - Arc\sin\left(\frac{a(1-\omega)}{C}\right)$$

3.2.2. Case a = b

If $a = b$, then point J does not exist because the outer common tangents of $\boldsymbol{C}_A$ and $\boldsymbol{C}_B$ are parallel. Point I is located at the midpoint of the turning centres: $I = (\frac{C}{2}, 0)$.

- If $\quad \frac{C}{1-\omega} \leqslant \frac{C}{2} \quad \Rightarrow \quad \frac{1}{1-\omega} \leqslant \frac{1}{2}$ (by $C > 0$)

  $$\Rightarrow \quad \frac{\pi}{2} + Arc\sin\left(\frac{b(\omega-1)}{C}\right) \leqslant \gamma \leqslant \frac{3\pi}{2} - Arc\sin\left(\frac{b(\omega-1)}{C}\right)$$

- If $\quad \frac{C}{2} \leqslant \frac{C}{1-\omega} \quad \Rightarrow \quad \frac{1}{2} \leqslant \frac{1}{1-\omega}$ (by $C > 0$)

  $$\Rightarrow \quad |\zeta| \leqslant \frac{\pi}{2} - Arc\sin\left(\frac{a(1-\omega)}{C}\right)$$

3.2.3. Case a > b

Finally, if $a > b$, the case may be developed in a similar fashion as the case for $a < b$.

3.3. Construction of the solution

In general we have one of two situations: either, for a given position of aircraft-B, P_B, the position of aircraft-A, P_A, can be constructed on $\boldsymbol{C}_A$ by the intersection of the straight line from position, P_B to F extrapolated to $\boldsymbol{C}_A$; or, alternatively, and similarly, for the case in which P_A is given, then the point P_B can be determined using the same approach by interchanging the roles of points P_A and P_B.

Recall that the domain for one of the angles in the pair (ζ, γ) is given directly. This domain is bounded by the two tangents constructed from the stationary fixed reference point $F = (\frac{C}{1-\omega}, 0)$ to a specified turning circle. We only need to construct the domain of the remaining angle based on the first known angle and the fixed reference point, F (see Fig. 3).

As an example, assume that $a \leqslant b$ and that F is located between the two fixed reference points I and J. That is: $\frac{1}{1-\frac{1}{r}} \leqslant \frac{1}{1-\omega} \leqslant \frac{1}{1+\frac{1}{r}}$.

The domain for the angle γ is determined from the bounds of two tangents constructed from F to $\boldsymbol{C}_B$:

$$\frac{\pi}{2} + Arc\sin\left(\frac{b(\omega-1)}{\omega C}\right) \leqslant \gamma \leqslant \frac{3\pi}{2} - Arc\sin\left(\frac{b(\omega-1)}{\omega C}\right)$$

Let

$$\gamma_T = \frac{\pi}{2} + Arc\sin\left(\frac{b(\omega-1)}{\omega C}\right)$$

We have

$$\frac{x_A - \frac{C}{1-\omega}}{x_B - \frac{C}{1-\omega}} = \frac{y_A}{y_B} \quad (\text{by similar triangles})$$

$$\Rightarrow \quad \frac{a\cos\zeta - \frac{C}{1-\omega}}{C + b\cos\gamma_T - \frac{C}{1-\omega}} = \frac{a\sin\zeta}{b\sin\gamma_T} \quad (\text{for the limiting case } \gamma = \gamma_T)$$

Clearly, this equation presented in the form of: $\alpha_0 + \alpha_1\cos\zeta + \alpha_2\sin\zeta = 0$, can be solved analytically. Let ζ_T be a root such that $0 < \zeta_T < \frac{\pi}{2}$, then the domain of ζ can be written as: $|\zeta| \leqslant \zeta_T$.

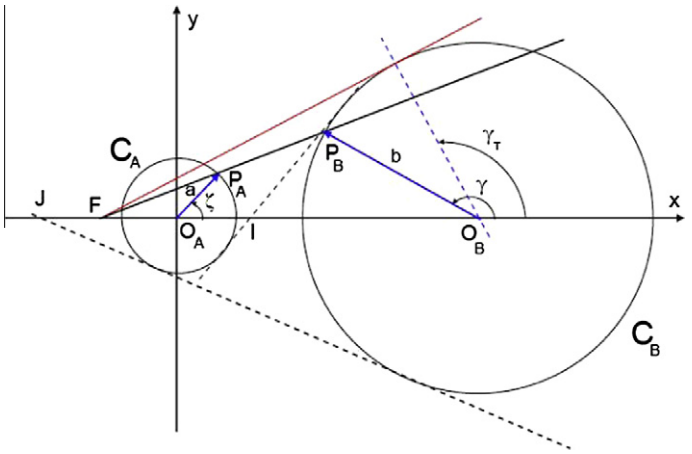

Fig. 3. Construction of domains, given the fixed reference point.

4. Categorisation of the minima

In this section, the four categories of minima are identified. Their specification is based on Eq. (2) (or one of its simplified forms) and formulated as an analytical geometry result. The categories are referenced as M_0, M_1, M_2 and M_3. The possible solutions are now described.

4.1. Global minima (M_0)

The global minimum occurs at the minimum physical distance between the turning circles. Hence, the principal domain value of the global minimum is: $(\zeta^*, \gamma^*) = (0, \pi)$.

A phase map of (ζ, γ) can be constructed by writing the equations for ζ and γ in terms of the rotational velocities and initial phase shifts.

$$\begin{cases} \zeta = \omega_A t + \zeta_0 \\ \gamma = \omega_B t + \gamma_0 \end{cases} \quad \Rightarrow \quad \frac{\gamma - \gamma_0}{\omega_B} = \frac{\zeta - \zeta_0}{\omega_A} \quad \Rightarrow \quad \zeta = \frac{\omega_A}{\omega_B}(\gamma - \gamma_0) + \zeta_0$$

Then the value of γ when $\zeta = 0$ is given by:

$$\frac{\omega_A}{\omega_B}(\gamma - \gamma_0) + \zeta_0 = 0 \quad \Rightarrow \quad \gamma|_{\zeta=0} = \gamma_0 - \frac{\omega_B}{\omega_A}\zeta_0$$

The global minimum exists for the following condition:

$$\gamma_0 - \frac{\omega_B}{\omega_A}\zeta_0 = \pi \text{ or } \gamma_0 = \frac{\zeta_0}{\omega} + \pi \quad \text{where} \quad \omega = \frac{\omega_A}{\omega_B}$$

In flight this condition can be tested when the rate of change of heading of each aircraft and the initial phase angles on the respective turn circles are known. The condition can be constantly recomputed and checked as the turn rates, speeds and even turn radii change throughout the manoeuvres.

4.2. Parallel minima (M_1)

The parallel minimum occurs when the vector rotational velocities are equal, i.e., $\underline{\omega}_A = \underline{\omega}_B$. The two aircraft will move with generally opposite linear velocity vectors within the collision zone. Hence, the comparative rate of change of relative range contributed by both aircraft on $R^2(\zeta, \gamma)$ can be approximated as the sum of differential rates from each aircraft moving on their respective turning circles according to the variables ζ and γ. The equivalent equation of the stationary points, for the whole system, is then represented by:

$$\frac{\partial R^2}{\partial \zeta} + \frac{\partial R^2}{\partial \gamma} = 0$$

Clearly, for this case, where $\omega = 1$ Fermat's vector equation (Eq. (2)) can be written as:

$$\underline{C} \times \underline{R} = 0$$

Interpreted geometrically, this is the case where the vector $\underline{R}$ is parallel to $\underline{C}$ (on the X-axis). Thus, the slope of $\underline{R}$ is zero.

$$\Rightarrow \quad \frac{b\sin\gamma - a\sin\varsigma}{b\cos\gamma - a\cos\varsigma} = 0$$

$$\Rightarrow \quad a\sin\zeta = b\sin\gamma \quad \text{where} \begin{cases} \zeta = \omega_A t + \zeta_0 \\ \gamma = \omega_B t + \gamma_0 \end{cases} \text{(with } \omega_A = \omega_B\text{)}$$

$$\Rightarrow \quad \frac{\sin\zeta}{\sin\gamma} = \frac{b}{a} = m = \frac{1}{r} \quad \text{(a constant)}$$

Applying the identity on fractions (addition or subtraction of the numerators and the denominators of equal fractions to obtain a new but equal fraction) yields:

$$\frac{\sin\zeta}{m} = \frac{\sin\gamma}{1} = \frac{\sin\zeta - \sin\gamma}{m-1} = \frac{\sin\zeta + \sin\gamma}{m+1}$$

$$\Rightarrow \quad \frac{\sin\zeta - \sin\gamma}{\sin\zeta + \sin\gamma} = \frac{m-1}{m+1} = \frac{1-r}{1+r}$$

Use the identities for the sum and differences of sines:

$$\frac{\sin\zeta - \sin\gamma}{\sin\zeta + \sin\gamma} = \frac{2\sin\left(\frac{\zeta-\gamma}{2}\right)\cos\left(\frac{\zeta+\gamma}{2}\right)}{2\sin\left(\frac{\zeta+\gamma}{2}\right)\cos\left(\frac{\zeta-\gamma}{2}\right)} = \frac{1-r}{1+r}$$

$$\Rightarrow \quad \frac{\tan\left(\frac{\zeta-\gamma}{2}\right)}{\tan\left(\frac{\zeta+\gamma}{2}\right)} = \frac{1-r}{1+r}$$

$$\Rightarrow \quad \tan\left(\frac{\zeta+\gamma}{2}\right) = \frac{1+r}{1-r}\tan\left(\frac{\zeta-\gamma}{2}\right) \quad \text{provided } r \neq 1$$

Because the turn rates are equal with the same sign:

$$\omega = 1 \quad \Rightarrow \quad \omega_A = \omega_B \quad \Rightarrow \quad \zeta - \gamma = \zeta_0 - \gamma_0 \quad \text{(it is a constant)}$$

$$\Rightarrow \quad \tan\left(\frac{\zeta+\gamma}{2}\right) = \frac{1+r}{1-r}\tan\left(\frac{\zeta_0-\gamma_0}{2}\right) \quad \text{provided } r \neq 1$$

The RHS is known. Then $\tan\alpha$, in this case, is given by:

$$\tan\left(\frac{\zeta+\gamma}{2}\right) = \tan\alpha \quad \text{where } \alpha = Arc\tan\left(\frac{1+r}{1-r}\tan\left(\frac{\zeta_0-\gamma_0}{2}\right)\right)$$

$$\Rightarrow \quad \zeta + \gamma = 2\alpha + 2k\pi \text{ for } k = 0, \pm1, \pm2, \pm3, \ldots$$

Thus

$$\begin{cases} \zeta = \alpha + \frac{\zeta_0-\gamma_0}{2} + k\pi \\ \gamma = \alpha - \frac{\zeta_0-\gamma_0}{2} + k\pi \end{cases} \quad \text{for } k = 0, \pm1, \pm2, \pm3, \ldots$$

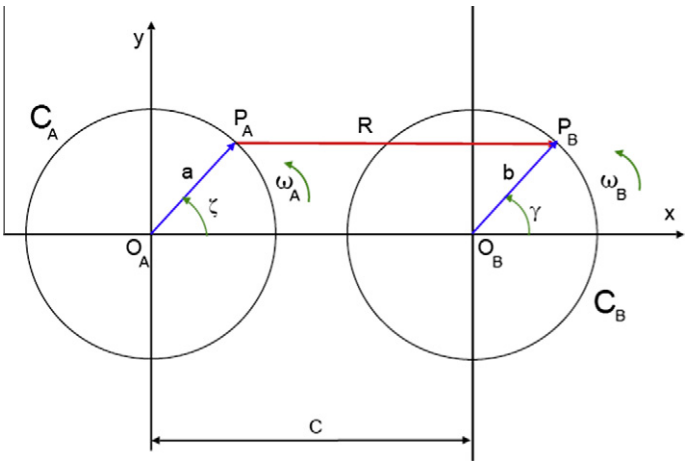

Fig. 4. Case for $\omega_A = \omega_B$ and $r = 1$.

$$\Rightarrow \quad t = \frac{2\alpha - (\zeta_0 + \gamma_0) + 2k\pi}{2\omega_A} = \frac{2\alpha - (\zeta_0 + \gamma_0) + 2k\pi}{2\omega_B} \quad \text{for } k = 0, \pm 1, \pm 2, \pm 3, \ldots$$

In the case $r = 1$, then $\tan\left(\frac{\zeta-\gamma}{2}\right) = 0$, thus $\zeta = \gamma$ and $\zeta_0 = \gamma_0$ (by $\omega_A = \omega_B$), as shown in Fig. 4, the relative range between aircraft will remain constant if the aircraft are in phase, and so there are an infinite number of solutions to the equation.

(Section 4.4 considers the case where the aircraft are not in phase.)

4.3. Radial minima (M_2)

Consider now the cases for which one aircraft turns more rapidly compared with the other aircraft. The domain for ω partitions into four regimes delimited by $\omega = \pm 1$ and characterised by $|\omega_A| \ll |\omega_B|$ and $|\omega_B| \ll |\omega_A|$. Each regime has a limiting case for which a radial minimum occurs. The limiting cases in terms of aircraft turn rate are either $|\omega_B| = 0 \Leftrightarrow |\omega| = \infty$ or $|\omega_A| = 0 \Leftrightarrow \omega = 0$. For each of the limiting cases in each regime the whole differential rate, for $R^2(\zeta,\gamma)$, can be approximated by the differential rate for the faster turning aircraft alone as it moves on its turning circle. For example, in the regimes for which $|\omega_A|$ becomes very large compared with $|\omega_B|$ ($|\omega_B| \ll |\omega_A|$), when aircraft-$A$ is turning rapidly, the equivalent equation for the stationary points for the whole system can be written simply as:

$$\frac{\partial R^2}{\partial \zeta} = 0$$
$$\Rightarrow \quad \frac{\partial R^2}{\partial \zeta} = 2ab\sin(\zeta - \gamma) + 2aC\sin\zeta = 0$$
$$\Rightarrow \quad b\sin(\zeta - \gamma) + C\sin\zeta = 0 \quad (a \neq 0)$$

The limiting case for this regime is $\omega_B = 0$, and Eq. (3) becomes: $\underline{a} \times \underline{R} = 0$. The geometrical interpretation of this expression shows that the positions of the two aircraft (points P_A, P_B) and the centre of turning circle O_A are collinear at the minimum, see Fig. 5.

A second regime is when $|\omega_A| \ll |\omega_B|$ and aircraft-B is turning more rapidly compared to aircraft-A. Now the whole differential rate, for $R^2(\zeta,\gamma)$, can be approximated by the differential turn rate of aircraft-B alone. The equivalent equation of stationary points for the whole system is:

$$\frac{\partial R^2}{\partial \gamma} = 0$$
$$\Rightarrow \quad \frac{\partial R^2}{\partial \gamma} = 2ab\sin(\zeta - \gamma) + 2bC\sin\gamma = 0$$
$$\Rightarrow \quad a\sin(\zeta - \gamma) + C\sin\gamma = 0 \quad (b \neq 0)$$

The limiting case for this regime is given by $\omega_A = 0$. Fermat's vector equation (Eq. (2)) becomes: $(\underline{a} - \underline{C}) \times \underline{R} = 0$. Clearly, P_A, P_B and O_B are collinear.

The third and fourth regimes can be treated similarly.

In summary, case M_2 is characterized by P_A, P_B and the centre of one of the turning circles being collinear. Mathematically,

$$\underline{a} \times \underline{R} = 0 \quad \text{for } P_A,\ P_B \text{ and } O_A \text{ collinear.}$$

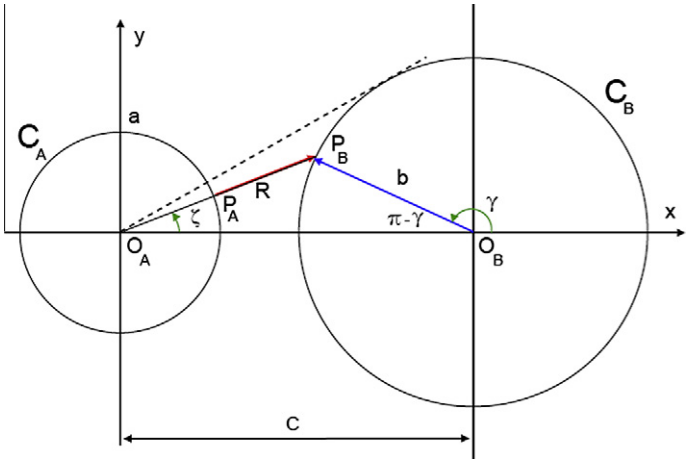

Fig. 5. The radial minima.

or

$$(\underline{a}-\underline{C})\times\underline{R}=0 \text{ for } P_A,\ P_B \text{ and } O_B \text{ collinear.}$$

Now, consider the case for P_A, P_B and O_A collinear:

$$\Rightarrow \quad b\sin(\zeta-\gamma)+C\sin\zeta=0$$

In this case: $\omega_A = 0$, the above equation reduces to:

$$b\sin(-\omega_B t+\zeta_0-\gamma_0)+C\sin\zeta_0=0$$
$$\Rightarrow \quad \sin(-\omega_B t+\zeta_0-\gamma_0)=-\frac{C}{b}\sin\zeta_0 \quad \text{(a constant)}$$

Therefore,

$$t=\frac{(-1)^{k+1}Arc\sin\left(-\frac{C}{b}\sin\zeta_0\right)-\zeta_0+\gamma_0+k\pi}{\omega_B} \quad \text{for } k=0,\pm1,\pm2,\pm3,\ldots$$

If $\omega_B = 0$, then $b\sin(\omega_A t+\zeta_0-\gamma_0)+C\sin(\omega_A t+\zeta_0)=0$

$$\Rightarrow \qquad \sin^2(\omega_A t+\zeta_0)=\frac{b^2\sin^2\gamma_0}{b^2+C^2+2bC\cos\gamma_0} \quad \text{(a constant)}$$

Therefore,

$$t=\frac{(-1)^k Arc\sin\left(\pm\frac{b|\sin\zeta_0|}{\sqrt{b^2+C^2+2bC\cos\gamma_0}}\right)-\zeta_0+k\pi}{\omega_A} \quad \text{for } k=0,\pm1,\pm2,\pm3,\ldots$$

4.4. Transverse minima (M_3)

Finally, a transverse minimum occurs for cases which are not: the parallel case ($\underline{\omega_A}=\underline{\omega_B}$); or the radial cases (either $\omega_B = 0 \Leftrightarrow |\omega| = \infty$ or for $|\omega_A| = 0 \Leftrightarrow \omega = 0$). Recall that here ω is finite and $\omega \neq 1$. Eq. (3) reduces to Eq. (4):

$$\left[\left(\frac{1}{1-\omega}\right)\underline{C}-\underline{a}\right]\times\underline{R}=0$$

Thus, the straight lines generated by vectors $\underline{R}$ and $\underline{C}$ are transverse and intersect at the fixed reference point $(\frac{C}{1-\omega},0)$. The equivalent equation for stationary points for the whole system is represented by:

$$\frac{\partial R^2}{\partial\zeta}\omega+\frac{\partial R^2}{\partial\gamma}=0$$
$$\Rightarrow \quad 2\omega(ab\sin(\zeta-\gamma)+aC\sin\zeta)-2(ab\sin(\zeta-\gamma)+bC\sin\gamma)=0$$
$$\Rightarrow \quad (\omega-1)ab\sin(\zeta-\gamma)+C(\omega a\sin\zeta-b\sin\gamma)=0 \quad \text{where } \begin{cases}\zeta=\omega_A t+\zeta_0\\ \gamma=\omega_B t+\gamma_0\end{cases}$$

In this general case it appears that a numerical solution is required.

A special case is when $\omega_A = -\omega_B$, then $\omega = -1$. The two aircraft will be moving in approximately the same general direction within the collision zone (but inverse angular velocities). Hence, the relative rate of change of $R^2(\zeta,\gamma)$ for the whole system is equivalent to the difference of the differential rates in relative range contributed by each aircraft moving around its turning circle. The equivalent equation of the stationary points for the whole system is then represented by:

$$\frac{\partial R^2}{\partial\zeta}-\frac{\partial R^2}{\partial\gamma}=0$$

$$\Rightarrow \quad 4ab\sin(\zeta-\gamma)+2C(a\sin\zeta+b\sin\gamma)=0$$

In this particular case, the fixed reference point is $(\frac{\zeta}{2},0)$. Therefore, vector $\underline{R}$ crosses at the midpoint between the turning centres, as shown in Fig. 6. Mathematically,

$$2ab\sin(\zeta-\gamma)+C(a\sin\zeta+b\sin\gamma)=0 \quad \text{where } \begin{cases}\zeta=\omega_A t+\zeta_0\\ \gamma=\omega_B t+\gamma_0\end{cases} \text{ (with } \omega_A=-\omega_B)$$

$$\Rightarrow \quad 2ab\sin(2\omega_A t+\zeta_0-\gamma_0)+C\{a\sin(\omega_A t+\zeta_0)+b\sin(-\omega_A t+\gamma_0)\}=0$$

This equation may be solved analytically by a transformation into a cubic equation. First, rewrite the equation into the form of:

$$c_0 + c_1 \sin\varphi + c_2 \cos\varphi + c_3 \sin\varphi \cos\varphi = 0$$

The constants c_0, c_1, c_2 and c_3 are determined by use of a new variable: $\varphi = \omega_A t = -\omega_B t$

Second, a cubic equation is obtained in terms of the variable τ, by using the following three transformations: $\tau = \tan\frac{\varphi}{2}$; $\sin\varphi = \frac{2\tau}{1+\tau^2}$ and $\cos\varphi = \frac{1-\tau^2}{1+\tau^2}$.

Clearly, in this particular form, the equation can again be solved analytically.

In summary, categories for the minima versus characteristics of (r,ω) are shown in Table 1.

5. Sufficient condition for determination of aircraft miss-distances

In this section, a sufficient condition for the minimum aircraft-to-aircraft miss-distance is found.

5.1. Derivation of the sufficient condition

The squared relative range, R^2 is given in Eq. (1) as:

$$R^2 = C^2 + a^2 + b^2 - 2Ca\cos\zeta + 2Cb\cos\gamma - 2ab\cos(\zeta-\gamma) \quad \text{where} \begin{cases} \zeta = \omega_A t + \zeta_0 \\ \gamma = \omega_B t + \gamma_0 \end{cases}$$

$$\Rightarrow \quad \frac{1}{2}\frac{dR^2}{dt} = \omega_A(ab\sin(\zeta-\gamma) + aC\sin\zeta) - \omega_B(ab\sin(\zeta-\gamma) + bC\sin\gamma)$$

$$\Rightarrow \quad \frac{1}{2}\frac{d^2R^2}{dt^2} = \omega_A^2[ab\cos(\zeta-\gamma) + aC\cos\zeta] - 2\omega_A\omega_B ab\cos(\zeta-\gamma) + \omega_B^2[ab\cos(\zeta-\gamma) - bC\cos\gamma]$$

$$\Rightarrow \quad \frac{1}{2\omega_B^2}\frac{d^2R^2}{dt^2} = (1-\omega)^2 ab\cos(\zeta-\gamma) + \omega^2 aC\cos\zeta - bC\cos\gamma \text{ by } \omega = \frac{\omega_A}{\omega_B}$$

$$\Rightarrow \quad \frac{1}{2\omega_B^2}\frac{d^2R^2}{dt^2} = (1-\omega)^2(x_A(x_B - C) + y_A y_B) + \omega^2 C x_A - C(x_B - C)$$

$$\Rightarrow \quad \frac{1}{2\omega_B^2}\frac{d^2R^2}{dt^2} = (1-\omega)^2(x_A x_B + y_A y_B) + C[C + (2\omega - 1)x_A - x_B]$$

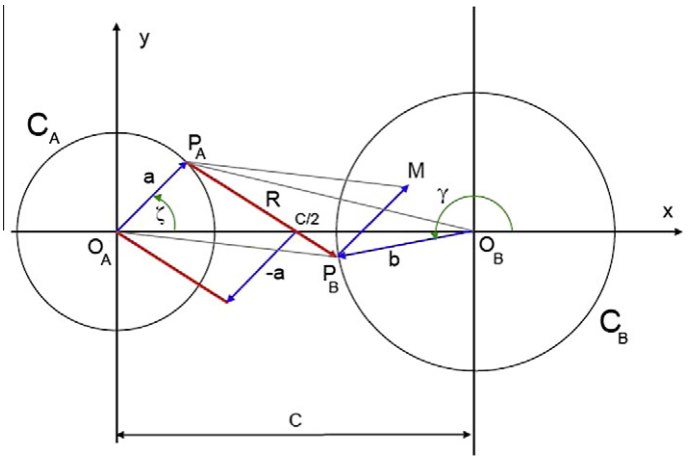

Fig. 6. The transverse minima.

Table 1
Type of minimum categorised according to (r,ω).

r	ω				
	$\omega = -\infty$	$\omega = -1$	$\omega = 0$	$\omega = 1$	$\omega = +\infty$
$r < 1$	$M_{0,2}$	$M_{0,3}$	$M_{0,2,3}$	$M_{0,1}$	$M_{0,2}$
$r = 1$	$M_{0,2}$	$M_{0,3}$	$M_{0,2,3}$	$M_{0,1}$	$M_{0,2}$
$r > 1$	$M_{0,2}$	$M_{0,3}$	$M_{0,2,3}$	$M_{0,1}$	$M_{0,2}$

The sufficient condition for minimising R^2 is: $\frac{d^2R^2}{dt^2} > 0$

$$\Rightarrow \quad (1-\omega)^2(x_Ax_B + y_Ay_B) + C[C + (2\omega - 1)x_A - x_B] > 0$$

$$\Rightarrow \quad x_Ax_B + y_Ay_B + \frac{C}{(1-\omega)^2}[C + (2\omega - 1)x_A - x_B] > 0 \quad \text{provided } \omega \neq 1$$

Let $u = \frac{C}{1-\omega}$. Thus, u is the X-coordinate of the fixed reference point F. Clearly, the position of point F, on the X-axis, is completely determined by u. In terms of u, the sufficient condition can be presented in the form of a quadratic expression:

$$C(x_Ax_B + y_Ay_B + u^2) + u(u - 2C)x_A - u^2x_B > 0$$

It suggests that the discriminant D, for this quadratic condition, can be used to determine the topologies of the trajectories of the two turning aircraft under the sufficient condition.

5.2. Operational regions for the point of closest approach

The possible regions for the point of closest approach between the two turning aircraft are determined by the three quantities: a, b and C. Consider the three possible cases:

(i) $a \leqslant C$ and $b \leqslant C$
(ii) $a > b > C$ or $a > C \geqslant b$
(iii) $b > C$ and $a \leqslant b$

5.2.1. The case of $a \leqslant C$ and $b \leqslant C$

In this case, the region in which the points of closest approach occur is located on the right hand side of the turning centre O_A and on the left hand side of the turning centre O_B. The special extreme case for R^2 occurs when both aircraft are located on the X axis: $\zeta = 0$ and $\gamma = \pi$, hence $x_A = a$, $x_B = C - b$ and $y_A = y_B = 0$. Thus, the sufficient condition becomes: $C(a(C-b) + u^2) + u(u - 2C)a - u^2(C - b) > 0$

This has a simple quadratic form (with respect to u) of:

$$(a+b)u^2 - 2aCu + aC(C-b) > 0$$

Let

$$Q = (a+b)u^2 - 2aCu + aC(C-b)$$

(Q is a quadratic polynomial with respect to the variable u)

Clearly, the sufficient condition will be satisfied, if: $Q > 0$. Consider all possible signs for Q by solving the quadratic equation: $Q = 0$

$$\Rightarrow \quad (a+b)u^2 - 2aCu + aC(C-b) = 0$$

Let D be the discriminant of the quadratic equation, thus

$$D = a^2C^2 - (a+b)aC(C-b) = abC(a+b-C)$$

- If $C > a + b$ (two circular trajectories of aircraft are separated) then the value of the discriminant is $D < 0$. Thus, the quadratic equation ($Q = 0$) has no solution. Furthermore, the quadratic coefficient of Q is positive (it equals $a + b$) thus implying that $Q > 0$.
- If $C = a + b$ (two circular trajectories of aircraft are touching) then the value of the discriminant is $D = 0$. Hence, the quadratic equation has a double root: $u_0 = \frac{aC}{a+b}$. Thus, $Q \geqslant 0$ (by the quadratic coefficient of Q is positive).
- If $C < a + b$ (two circular trajectories of aircraft are overlapping) then the value of the discriminant $D > 0$. Hence, the quadratic equation has two real roots:

$$u_1 = \frac{aC - \sqrt{D}}{a+b} \text{ and } u_2 = \frac{aC + \sqrt{D}}{a+b}$$

Therefore, $Q > 0$ for $u < u_1$ (or $u > u_2$). Otherwise, $Q \leqslant 0$ for $u_1 \leqslant u \leqslant u_2$.

5.2.2. The case of $a > b > C$ or $a > C \geqslant b$

Clearly, the region of closest points of approach is located on the right hand side of both circular trajectories. In the extreme case, put $\zeta = 0$ and $\gamma = 0$, hence $x_A = a$, $x_B = b + C$ and $y_A = y_B = 0$. Thus, the sufficient condition becomes:

$$C(a(b+C) + u^2) + u(u - 2C)a - u^2(b+C) > 0$$

This has a simple quadratic form (with respect to u) of:

$$(a-b)u^2 - 2aCu + aC(b+C) > 0$$

Let $Q = (a-b)u^2 - 2aCu + aC(b+C)$

(Q is a quadratic polynomial with respect to the variable u).

Similarly, the sufficient condition will be satisfied, if: $Q > 0$. Consider all possible signs for Q by solving the quadratic equation: $Q = 0$

$$\Rightarrow \qquad (a-b)u^2 - 2aCu + aC(b+C) = 0$$

Let D be the discriminant of the quadratic equation, thus

$$D = a^2C^2 - (a-b)aC(b+C) = abC(b+C-a)$$

- If $a > b + C$ (then one aircraft's circular trajectory lies inside the other aircraft's circular trajectory). The value of the discriminant is $D < 0$. Thus, the quadratic equation ($Q = 0$) has no solution. Furthermore, since the quadratic coefficient of Q ($a - b > 0$) this implies that $Q > 0$.
- If $a = b + C$ (two circular trajectories of aircraft are touching) then the value of the discriminant is $D = 0$. Hence, the quadratic equation has a double root: $u_0 = \frac{aC}{a-b}$. Thus, $Q \geqslant 0$ (by the quadratic coefficient of Q is positive).
- If $a < b + C$ (two circular trajectories of aircraft are overlapping) then the value of the discriminant is $D > 0$. Hence, the quadratic equation has two real roots:

$$u_1 = \frac{aC - \sqrt{D}}{a-b} \quad \text{and} \quad u_2 = \frac{aC + \sqrt{D}}{a-b} \quad \text{by } a > b$$

Therefore, $Q > 0$ for $u < u_1$ or $u > u_2$. Otherwise, $Q \leqslant 0$ for $u_1 \leqslant u \leqslant u_2$.

5.2.3. The case of $b > C$ and $a \leqslant b$

In this case, the closest points of approach are located on the left hand side of both circular trajectories. For the extreme cases, put $\zeta = \pi$ and $\gamma = \pi$, hence $x_A = -a$, $x_B = C - b$ and $y_A = y_B = 0$.

Thus, the sufficient condition becomes:

$$C(-a(C-b) + u^2) - u(u-2C)a - u^2(C-b) > 0$$

which has a simple quadratic form (with respect to u):

$$(b-a)u^2 + 2aCu + aC(b-C) > 0$$

Let $Q = (b-a)u^2 + 2aCu + aC(b-C)$

(Q is a quadratic polynomial with respect to the variable u).

Thus, the sufficient condition will be satisfied, if: $Q > 0$. Consider all possible signs for Q by solving the quadratic equation: $Q = 0$

$$\Rightarrow \quad (b-a)u^2 + 2aCu + aC(b-C) = 0$$

Let D be the discriminant of the quadratic equation, thus

$$D = a^2C^2 - (b-a)aC(b-C) = abC(a+C-b)$$

- If $b > a + C$ (one aircraft's circular trajectory lies inside the other aircraft's circular trajectory) then the value of the discriminant is $D < 0$. Thus, the quadratic equation ($Q = 0$) has no solution. Furthermore, if the quadratic coefficient of Q is positive (that is $a < b$) this implies that $Q > 0$. Otherwise, $Q < 0$ for $a > b$.
- If $b = a + C$ (two circular trajectories of aircraft are touching) then the value of the discriminant is $D = 0$. Hence, the quadratic equation has a double root: $u_0 = \frac{aC}{a-b}$. Thus, $Q \geqslant 0$ for $a < b$ or $Q < 0$ for $a > b$ (the quadratic coefficient of Q is either positive or negative).
- If $b < a + C$ (two circular trajectories of aircraft are overlapping) then the value of the discriminant is $D > 0$. Hence, the quadratic equation has two real roots:

$$u_1 = \frac{aC - \sqrt{D}}{b-a} \text{ and } u_2 = \frac{aC + \sqrt{D}}{b-a} \quad \text{provided } a \neq b$$

Therefore, if $a < b$ then $Q > 0$ for $u < u_1$ (or $u > u_2$). Thus, $Q \leqslant 0$ for $a < b$ and $u_1 \leqslant u \leqslant u_2$. Otherwise, $Q > 0$ for $a > b$ and $u_1 < u < u_2$. Hence, $Q \leqslant 0$ for $u < u_1$ (or $u > u_2$) and $a > b$.

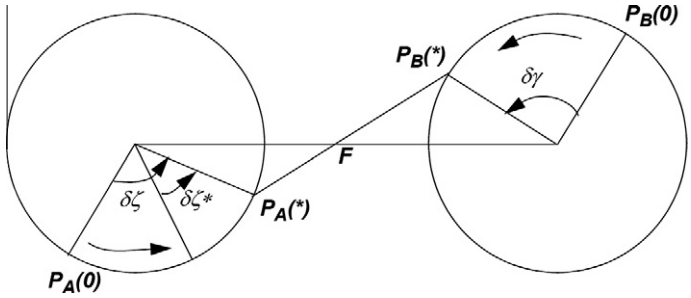

Fig. 7. Lead and lag for PCA.

6. Temporal dependencies

In this section the temporal aspects of the application of this methodology are illustrated. For each of three situations, the constants $\underline{\boldsymbol{O}}_{\boldsymbol{A}}$, $\boldsymbol{a}$, $\underline{\boldsymbol{O}}_{\boldsymbol{B}}$ and $\boldsymbol{b}$ (and by implication $\underline{\boldsymbol{C}}$) are all assumed to be known, thus the turn circles $\boldsymbol{C}_{\boldsymbol{A}}$ and $\boldsymbol{C}_{\mathrm{B}}$ are prescribed for aircraft-A and aircraft-B respectively.

6.1. Situation 1: Aircraft-A as reference

First consider that the aircraft are turning such that ω is negative and therefore $\boldsymbol{F}$ is located on the interior interval between turn centres. The condition under which a minima occurs is established through the theory presented, however, the phase relationship for which the minima occurs must be determined. Aircraft-A needs to determine where, along its turn circle, the minima in relative range will occur. The situation is specified by $\boldsymbol{P}_{\boldsymbol{A}}$, $\omega_{\boldsymbol{A}}$ and ω_B as known whereas $\boldsymbol{P}_{\boldsymbol{B}}{}^*$ is unknown.

The trajectory (path) of aircraft-A is taken as reference. The solution domain for the minima is a bounded arc of $\boldsymbol{C}_{\boldsymbol{A}}$. At any instant, given the positions of aircraft-A, $\boldsymbol{P}_{\boldsymbol{A}}(\boldsymbol{t})$ and $\boldsymbol{F}$, there corresponds a point $\boldsymbol{P}_{\boldsymbol{B}}{}^*(\boldsymbol{t})$ on $\boldsymbol{C}_{\mathrm{B}}$ that can be found through the condition of co-linearity for the minima. Considering successive instants establishes a locus of the optimum points for $\boldsymbol{P}_{\boldsymbol{B}}{}^*(\boldsymbol{t})$ on $\boldsymbol{C}_{\mathrm{B}}$ each of which is a candidate at which the minimum in relative range could occur. A second sequence is formed of successive instantaneous positions, $\boldsymbol{P}_{\boldsymbol{B}}(\boldsymbol{t})$, that locates the actual positions that Aircraft-B takes on $\boldsymbol{C}_{\mathrm{B}}$. The minima, denoted as $\boldsymbol{P}_{\boldsymbol{B}}{}^*$, will occur when, for a given instant of time t, the point $\boldsymbol{P}_{\boldsymbol{B}}{}^*(\boldsymbol{t})$ is coincident with the point $\boldsymbol{P}_{\boldsymbol{B}}(\boldsymbol{t})$.

6.2. Situation 2: Aircraft-B as reference

The converse to Situation 1 (with ω still negative) is one in which the locus of positions $\boldsymbol{P}_{\boldsymbol{B}}(\boldsymbol{t})$ is taken as a reference. Now the location of $\boldsymbol{P}_{\boldsymbol{A}}{}^*(\boldsymbol{t})$ that represents the minima in relative range is required. The method of solution is the same as Situation 1 but with the roles of the reference and intruder aircraft interchanged. In this situation $\boldsymbol{P}_{\boldsymbol{B}}$, ω_A and ω_B as known whereas $\boldsymbol{P}_{\boldsymbol{A}}{}^*$ is unknown.

6.3. Situation 3: Determine the Lead/Lag for the Point of Closest Approach

A third situation is where, at a time taken to be $t = 0$, the instantaneous positions of aircraft-A, $\boldsymbol{P}_{\boldsymbol{A}}(0)$, and of aircraft-B, $\boldsymbol{P}_{\boldsymbol{B}}(0)$ and its rotation rate, ω_B, are known. Also known are two critical points: $\boldsymbol{P}_{\boldsymbol{A}}(^*)$ and $\boldsymbol{P}_{\boldsymbol{B}}(^*)$, one on each trajectory. The objective is to determine the lag or lead of aircraft-A through $\boldsymbol{P}_{\boldsymbol{A}}(^*)$. This situation is illustrated in Fig. 7.

Given that positions $\boldsymbol{P}_{\boldsymbol{B}}(0)$ and $\boldsymbol{P}_{\boldsymbol{B}}(^*)$ are known then the change in heading, $\delta\gamma$, for aircraft-B can be found. Then the time δt for aircraft-B to reach $\boldsymbol{P}_{\boldsymbol{B}}(^*)$ is given by $\delta t = \frac{\delta\gamma}{\omega_B}$. Further given $\boldsymbol{P}_{\boldsymbol{A}}(^*)$ and $\boldsymbol{P}_{\boldsymbol{B}}(^*)$ are known then the fixed reference point, F, can be found which in turn permits the optimum turn rate ω_A^* to be found. Note that $\delta\zeta^* = \omega_A^* \cdot \delta t$. Now aircraft-A may not be at the position $\delta\zeta^*$ at $t = 0$ neither may it be travelling at ω_A^*. If the actual time of aircraft-A to reach $\boldsymbol{P}_{\boldsymbol{A}}(^*)$ is $\delta t = \frac{\delta\zeta}{\omega_A} = \frac{\delta\gamma}{\omega_B}$ then the prescribed minima in range occurs. If $\frac{\delta\zeta}{\omega_A} < \frac{\delta\gamma}{\omega_B}$ then aircraft-A passes through $\boldsymbol{P}_{\boldsymbol{A}}(^*)$ before aircraft-B passes through $\boldsymbol{P}_{\boldsymbol{B}}(^*)$. Conversely if $\frac{\delta\zeta}{\omega_A} > \frac{\delta\gamma}{\omega_B}$ the roles are reversed. The change of heading $\delta\zeta^*_{ref} = \omega_A \cdot \delta t$ can be used as a reference point in the turn for guiding aircraft-A.

7. Discussion and conclusion

The Point of Closest Approach (PCA) between two aircraft, each turning in a plane, has been studied for several decades. The earlier research based on a unity speed ratio had only identified a parallel minima ($\underline{\omega}_A = \underline{\omega}_B$) expressed as a relative heading of zero and transverse minima ($\underline{\omega}_A = -\underline{\omega}_B$) for pairwise turns with opposite angular directions. However the present research shows that in a more general situation there are four categories of minima: M0, the Global minima; M1, the Parallel minima; M2, the Radial minima; and M3, the Transverse minima.

A general vector equation characterising the minima has now been determined. The structure of the equation shows the strong dependency of the solution on the turn rate ratio, ω. Implicit in, and characterising the equation, is the identification of a fixed reference point, $\boldsymbol{F}$, that plays a central role in the geometric construction used to determine the location of the minima. The spatial location of $\boldsymbol{F}$ is on the vector joining the aircraft turn centres, or one of its extensions. The location of this point provides deeper geometric intuition for identifying the precise operational configuration under which the minimum will occur. This enables a more detailed classification of the type of minima to be encountered. Further classification is through the second order sufficiency condition which is shown to be characterised by relationships based on the norms of the two turn radii vectors and on the distance between turn centers.

Thus the Fermat vector equation and its associated geometrical constructions provide the means to more precisely specify and distinguish operational situations so that the nature of aircraft interaction in the turn can be uniquely categorised by reference to the classification of cases presented. This classification better facilitates the careful attention required in the design and test of proximity management systems. In practical applications the theory enables more detailed specification of designs and of the algorithms to be employed together with the ability to provide greater focus in specifying the domain coverage of the stress-testing strategies required for the verification and validation processes.

The rigorous mathematical solutions can also be used as the basis of developing higher level proofs based on formal methods approaches that are needed to assure that design implementations can achieved the level of integrity required. Such evidence is required in the presentation of safety cases associated with the development of navigation and guidance equipment used in the management of aircraft proximity that are part of the design of both the next generation air traffic management systems and of future aircraft avionics systems.

References

[1] N.L. Fulton, Airspace design: towards a rigorous specification of conflict complexity based on computational geometry, The Aeronautical Journal (1999).
[2] N.L. Fulton, Doctoral Dissertation, Regional Airspace Design: A Structured Systems Engineering Approach, University of New South Wales, 2002.
[3] A.W. Merz, Optimal Aircraft Collision Avoidance, In Proc. Joint Automatic Control Conference, Paper 15-3, 1973, pp. 449–454.
[4] A.W. Merz, Optimal evasive manoeuvres in maritime collision avoidance, Journal of the Institute of Navigation 20 (2) (1973) 144–152.
[5] A.J. Grunwald, Tunnel display for four-dimensional fixed-wing approaches, Journal of Guidance, Control and Dynamics, vol. 7, AIAA, 1984. 3, pp. 369–377.
[6] A.K. Barrows, P. Enge, B.W. Parkinson, J.D. Powell, Flying curved approaches and missed approaches: 3-D display trials onboard a light aircraft, in: Proc. ION GPS-96, Institute of Navigation (ION), Kansas City, Missouri, 1996.
[7] A.K. Barrows, K.W. Alter, P. Enge, B.W. Parkinson, J.D. Powell, Operational experience with and improvements to a tunnel-in-the-sky display for light aircraft, in: Proc. ION GPS-97, Institute of Navigation (ION), Kansas City, Missouri, 1997.
[8] K.W. Alter, A.K. Barrows, P. Enge, C.W. Jennings, B.W. Parkinson, J.D. Powell, Inflight demonstrations of curved approaches and missed approaches in mountainous terrain, in: Proc. ION GPS-98, Nashville, Institute of Navigation (ION), 1998.
[9] A.K. Barrows, K.W. Alter, C.W. Jennings, J.D. Powell, Alaskan flight trials of a synthetic vision system for instrument landings of a piston twin aircraft, in: Proc. SPIE Enhanced and Synthetic Vision, The International Society for Optical Engineering, 1999.
[10] A.K. Barrows, J.D. Powell, Tunnel-in-the-sky cockpit display for complex remote sensing flight trajectories, in: Proc. Fourth International Airborne Remote Sensing Conference and Exhibition/21st Canadian Symposium on Remote Sensing, Ottawa, Canada, 1999.
[11] M. Mulder, J.A. Mulder, H.G. Stassen, Cybernetics of the tunnel-in-the-sky displays, Part I: Straight trajectories, in: Proc. IEEE Systems, Man, and Cybernetics Conference (SMC'99), vol. 5, 12–15 Oct 1999, pp. 1088–1093.
[12] M. Mulder, J.A. Mulder, H.G. Stassen, Cybernetics of the tunnel-in-the-sky display, Part II: Curved tunnel trajectories, in: Proc. IEEE Systems, Man, and Cybernetics Conference (SMC'99), vol. 5, 12–15 October 1999, pp. 1082–1087.
[13] A.K. Barrows, J.D. Powell, Flying A Tunnel-in-the-Sky Display within the Current Airspace System, AIAA, 2000.
[14] R.L. Newman, M. Mulder, Pathway displays: A literature review, in: Proc. 22nd IEEE Digital Avionics System Conference (DASC '03), Indianapolis, IN, vol. 2, 12–16 October 2003.
[15] M. Mulder, H.J.C. van der Vaart, An information centred analysis of the tunnel-in-the-sky display, Part 3: Curve interception, International Journal of Aviation Psychology 16 (2006) 21–49.
[16] E. Theunissen, Towards a conceptual framework for comparing perspective flightpath displays, in: Proc. AIAA Flight Simulation Technologies Conference, AIAA-1996-3552, San Diego, CA, July 1996, pp. 29–31.
[17] E. Theunissen, R.M. Rademaker, T.J. Etherington, Synthetic vision-the display concept of the collins team, in: Proc. 20th IEEE Conference on Digital Avionics Systems, Daytona Beach Florida, 14–18 October 2001, vol. 1, pp. 2C2/1–2C2/8.
[18] S. Sachs, R. Sperl, Experimental low cost 3D display for general aviation aircraft, in: Proc. AIAA Atmospheric Flight Mechanics Conference and Exhibit, Montreal, Canada, August 2001, pp. 6–9.
[19] A.L. Alexander, C.D. Wickens, 3D Navigation and Integrated Hazard Display in Advanced Avionics: Performance, Situational Awareness, and Workload, Technical Report AHFD-05-10/NASA-05-2, NASA Langley Research Center, Hampton, VA, June 2005.
[20] M. Christodoulou, Automatic commercial aircraft-collision avoidance in free flight: the three-dimensional problem, IEEE Transactions on Intelligent Transportation Systems 7 (2) (2006) 242–249.
[21] H-N. Huynh, N. Fulton, Aircraft proximity termination conditions for 3D turn centric modes, Applied Mathematical Modelling 36 (2) (2012) 521–544, doi:10.1016/j.apm.2011.07.046.
[22] T. Miloh, M. Pachter, Ship collision-avoidance and pursuit-evasion differential games with speed-loss in a turn, Computers & Mathematics with Applications 18 (1–3) (1989) 77–100.
[23] J.K. Kuchar, L.C. Yang, A survey of conflict detection and resolution modeling methods, in: Proc. AIAA Guidance, Navigation and Control Conference, AIAA-97-3732, New Orleans, LA, August 1997, pp. 1388–1397.
[24] J.C. Clements, The optimal control of collision avoidance trajectories in air traffic management, Transportation Research Part B 33 (1999) 265–280.
[25] A. Miele, T. Wang, C.S. Chao, J.B. Dabney, Optimal control of a ship for course change and sidestep maneuvers, Journal of Optimization Theory and Applications, vol. 103, Springer, 1999. 2, pp. 259–282.
[26] A. Miele, T. Wang, C.S. Chao, J.B. Dabney, Optimal control of a ship for collision avoidance maneuvers, Journal of Optimization Theory and Applications, vol. 103, Springer, 1999. 3, pp. 495–518.
[27] J.K. Kuchar, L.C. Yang, A review of conflict detection and resolution modeling methods, IEEE Transactions on Intelligent Transportation Systems 1 (4) (2000) 179–189.
[28] J.C. Clements, Optimal simultaneous pairwise conflict resolution maneuvers in air traffic management, Journal of Guidance, Control and Dynamics, vol. 25, AIAA, 2002. 4, pp. 815–818.

[29] J. Hu, M. Prandini, S. Sastry, Optimal coordinated maneuvers for three-dimensional aircraft conflict resolution, Journal of Guidance, Control and Dynamics, vol. 25, AIAA, 2002. 5, pp. 888–900.
[30] R. Paielli, Modelling maneuver dynamics in air traffic conflict resolution, Journal of Guidance, Control and Dynamics, vol. 26, AIAA, 2003. 3, pp 407–415.
[31] A.U. Raghunathan, V. Gopal, D. Subramanian, L.T. Biegler, T. Samad, Dynamic optimization strategies for three-dimensional conflict resolution of multiple aircraft, Journal of Guidance, Control and Dynamics, vol. 27, AIAA, 2004. 4, pp. 586–594.
[32] A. Miele, T. Wang, Optimal trajectories and guidance schemes for ship collision avoidance, Journal of Optimization Theory and Applications, vol. 129, Springer, 2006. 1, pp. 1–20.
[33] C.L. Britt, J. Schrader, A statistical evaluation of aircraft collision hazard warning system techniques in the terminal area, IEEE Transactions on Aerospace and Electronic Systems AES-6 (1) (1970) 10–21.
[34] R.Y. Gazit, J.D. Powell, Aircraft collision avoidance based on GPS position broadcasts, in: Proc. 15th AIAA/IEEE Digital Avionics Systems Conference, 27–31 October 1996, pp. 393–399.
[35] K. Zeghal, A comparison of different approaches based on force fields for coordination among multiple mobiles, in: Proc. IEEE/RSJ International Conference on Intelligent Robots and Systems, vol. 1, 13–17 October 1998, pp. 273–278.
[36] T. Tarnopolskaya and N. Fulton, Optimal cooperative collision avoidance strategy for coplanar encounter: Merz's solution revisited, Journal of Optimization Theory and Applications, Springer, 2008.
[37] T. Tarnopolskaya, N. Fulton, Synthesis of optimal control for cooperative collision avoidance strategies for aircraft (ships) with unequal turn capabilities, Journal of Optimization Theory and Applications, Springer, 2008.
[38] H.-N. Huynh, N.L. Fulton, Proximity termination conditions for two aircraft: one with circular and one with straight uniform motion, in: R.S. Anderssen, R.D. Braddock, L.T.H. Newham (Eds.), 18th World IMACS Congress and MODSIM09 International Congress on Modelling and Simulation. Modelling and Simulation Society of Australia and New Zealand and International Association for Mathematics and Computers in Simulation, July 2009, pp. 411–417. ISBN: 978-0-9758400-7-8.
[39] S. Park, J. Deyst, J.P. How, A new nonlinear guidance logic for trajectory tracking, in: Proc. AIAA Guidance, Navigation and Control Conference and Exhibit, American Institute of Aeronautics and Astronautics, AIAA-2004-4900, Providence, Rhode Island, 16–19 August 2004, pp. 1–16.
[40] W.W.R. Ball, A Short Account of the History of Mathematics, Dover Publications, Inc., New York, 1960.
[41] M.S. Mahoney, The Mathematical Career of Pierre de Fermat, Princeton University Press, 1973.
[42] Paolini. PlanetMath: Fermat's Theorem (Stationary points). <http://planetmath.org/encyclopedia/FermatsTheoremStationaryPoints.html>, 2003.
[43] V. Sanford, A Short History of Mathematics, The Riverside Press, Cambridge–Massachusetts, 1930.
[44] P.H. Zipfel, Modeling and Simulation of Aerospace Vehicle Dynamics, AIAA Education Series, American Institute of Aeronautics and Astronautics, Reston, VA, 2000.
[45] G.W. Caunt, An Introduction to the Infinitesimal Calculus, Oxford at the Clarendon Press, London, 1946.
[46] H. Lamb, An Elementary Course of Infinitesimal Calculus, Cambridge University Press, London, 1961.
[47] R.F. Matlak, Functions of two or more variables, in: A. Keane, S.A. Senior (Eds.), Mathematical Methods, Science Press, Sydney, 1961.